UNDRAINED SHEAR STRENGTH OF LIQUEFIED SANDS FOR STABILITY ANALYSIS

By Timothy D. Stark,[1] Associate Member, ASCE and Gholamreza Mesri,[2] Member, ASCE

ABSTRACT: The postliquefaction shear strength of sands, called the undrained critical strength or s_u(critical), is evaluated in terms of the critical strength ratio, s_u(critical)/σ'_{vo}. This allows postliquefaction stability analyses to incorporate the variation of s_u(critical) with effective vertical stress instead of using a single value as proposed elsewhere. Comparison of back-calculated critical strength ratios and the cyclic stress ratios triggering liquefaction suggests that drainage occurs in most cases during the postliquefaction flow of liquefied sands. To evaluate the stability of an existing slope that is predicted to liquefy during a dynamic event, the original slope configuration and the constant volume s_u(critical) must be used instead of the back-calculated partially drained s_u(critical) values. The proposed procedure for estimating the constant volume s_u(critical), using the results of field and/or laboratory tests, shows that the critical strength ratio is approximately one-half the yield strength ratio at the triggering of liquefaction for an earthquake magnitude of 7.5. It has been shown that the yield strength ratio at the triggering of liquefaction for a magnitude of 7.5 can be estimated by 0.011 times the equivalent clean sand blow count. Therefore, the critical strength ratio is 0.0055 times the equivalent clean sand blow count.

INTRODUCTION

The undrained behavior of a loose cohesionless soil is illustrated by the consolidated-undrained triaxial compression test results shown in Fig. 1. The monotonic loading test was performed on a uniform, clean, fine quartz sand, referred to as a banding sand (Castro 1969). The test specimen was initially consolidated to an equal all-around pressure σ'_{3c} of approximately 400 kPa (8,350 psf). The minimum and maximum void ratios of the sand are 0.50 and 0.84. The void ratio of the specimen after consolidation was 0.71, which corresponds to a relative density of 37%. The specimen exhibited an undrained yield strength s_u(yield) of approximately 115 kPa (2,400 psf) at an axial strain of approximately 1%. After the yield strength was mobilized and the specimen liquefied, it deformed from an axial strain of about 1% to 19% in just 0.18 s.

At an axial strain of approximately 10%, the deviator stress and pore-water pressure became essentially constant. The postliquefaction shear strength, called the undrained critical strength s_u(critical) is approximately 40 kPa (835 psf). This critical strength was first defined by Casagrande (1936) while developing the critical void ratio concept. The undrained critical strength is the strength available after liquefaction has been triggered and is applicable to postliquefaction stability analyses. This paper reviews the current procedures for estimating the undrained shear strength of liquefied sands and then proposes a new approach for estimating s_u(critical).

[1]Asst. Prof. of Civ. Engrg., Univ. of Illinois, Newmark Civ. Engrg. Lab. MC-250, 205 N. Mathews Ave., Urbana, IL 61801.
[2]Prof. of Civ. Engrg., Univ. of Illinois, Urbana, IL.

Note. Discussion open until April 1, 1993. To extend the closing date one month, a written request must be filed with the ASCE Manager of Journals. The manuscript for this paper was submitted for review and possible publication on September 20, 1991. This paper is part of the *Journal of Geotechnical Engineering*, Vol. 118, No. 11, November, 1992. ©ASCE, ISSN 0733-9410/92/0011-1727/$1.00 + $.15 per page. Paper No. 2613.

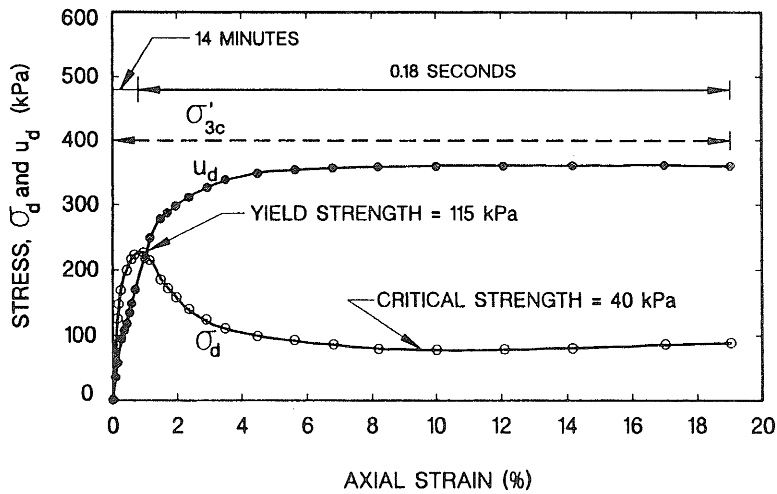

FIG. 1. Typical Stress-Strain Curves from Consolidated-Undrained Triaxial Compression Tests on Loose Sand [from Castro (1969)]

Critical Strength from Laboratory Tests and In Situ Void Ratio

Poulos et al. (1985) have developed a procedure for estimating the undrained shear strength of liquefied soils using the results of monotonically loaded, consolidated-undrained triaxial compression tests with pore-water pressure measurements on undisturbed and reconstituted soil samples. Fig. 2 shows this procedure for estimating the undrained critical strength from laboratory triaxial compression tests. The undrained critical strength is termed steady-state strength by Poulos et al. (1985) and residual strength by Seed (1987). The test results from reconstituted specimens are used to determine a relationship between undrained critical strength and void ratio. This critical-strength line is used to adjust the results of tests on undisturbed specimens for densification during sampling, handling, transportation, laboratory preparation, and laboratory consolidation. The undrained critical strength corresponding to the in situ void ratio is estimated by drawing a line through the laboratory void-ratio–critical-strength data point, parallel to the critical strength line. This technique assumes: (1) That the slope of the critical strength line is the same for reconstituted and undisturbed samples; and (2) that the slope of the critical strength line is independent of the method used to reconstitute the samples in the laboratory.

As Poulos et al. (1985) pointed out, the slope of the critical-strength line is mainly affected by the shape of the grains in a given soil, while the vertical position of the critical strength line is affected by small differences in grain-size distribution. However, recent studies by Vaid and Chern (1985), Vaid et al. (1990), and Konrad (1990a, b) indicate that the critical-strength line may be influenced by the mode of shear and the effective confining pressure. Dennis (1988) also states that sample preparation technique and method of loading, i.e., strain-controlled versus stress-controlled, affect the critical strength line.

A recent reevaluation of the slide in the upstream slope of the Lower San Fernando Dam provides a means for evaluating the Poulos et al. (1985)

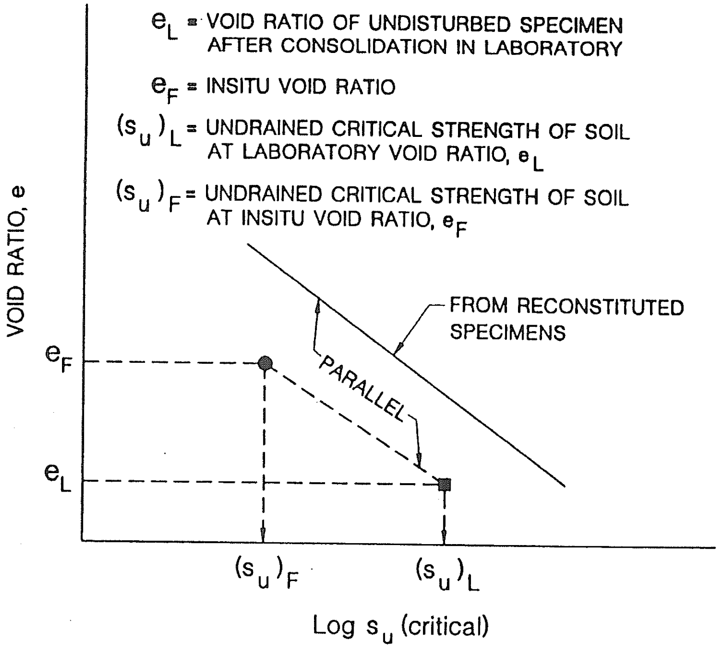

FIG. 2. Poulos et al. (1985) Procedure for Determining Undrained Critical Strength for Soil at In Situ Void Ratio

procedure. During the field investigation of the downstream shell, it was determined that a sandy silt, termed bulk sample 7, was representative of the hydraulic fill that liquefied in the upstream shell during the 1971 San Fernando, California, earthquake. Fig. 3 shows the critical strengths measured using monotonically loaded, consolidated-undrained triaxial compression tests on reconstituted and undisturbed specimens of the sandy silt by four different laboratories. These laboratories included the Corps of Engineers Waterways Experiment Station (WES) (Marcuson et al. 1990); GEI Consultants, Inc., Winchester, Massachusetts (Castro et al. 1989), Rensselaer Polytechnic Institute (RPI) (Vasquez-Herrera and Dobry 1989), and Stanford University (Seed et al. 1989). The median grain size, D_{50}, of the sandy silt of the reconstituted specimens is 0.07 mm, and those of the undisturbed specimens are in the range of 0.02–0.2 mm. The coefficient of uniformity and fines content, i.e., percent passing the No. 200 sieve, of the reconstituted specimens are 18 and 48%, respectively. The undisturbed specimens have a coefficient of uniformity ranging from 6 to 100 and a fines content ranging from 22% to 90%. Since there is no significant difference between the average gradation curve and fines content for the undisturbed and reconstituted specimens, the major difference in the critical strengths at a given void ratio was explained by Marcuson et al. (1990) in terms of the stratified nature of the undisturbed specimens. In other words, a grain-size analysis of the whole specimen may not properly represent the gradation and fines content of a stratification that may control the undrained critical strength of the undisturbed specimen. However, the fact that the undisturbed critical strengths all plot above the critical-strength line of reconsti-

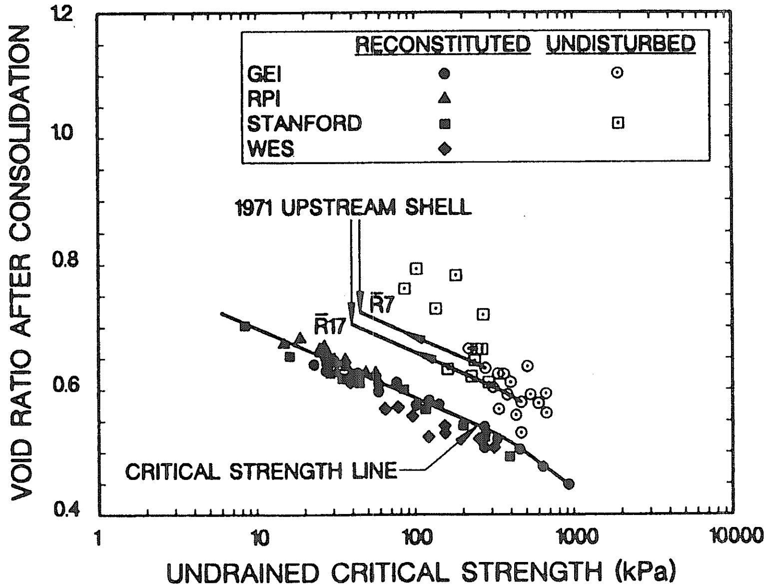

FIG. 3. Undrained Critical Strength of Sandy Silt from Lower San Fernando Dam, Sampled and Tested in 1985 [from Marcuson et al. (1990)]

tuted specimens suggests that factors other than gradation may influence the location of the critical strength line. These factors may include initial soil structure, mode of shear, and effective confining pressure.

Equal all-around consolidation pressures in the range of 40–3,200 kPa (835–66,830 psf) were used for the undrained shear tests on reconstituted specimens of the sandy silt, whereas the consolidation pressure range for the undisturbed specimens was 300–1,200 kPa (6,265–25,000 psf). The values of undrained critical strength at the after-consolidation void ratio range from 87 to 670 kPa (1,820 to 14,000 psf). The undrained critical strengths were corrected to the pre-earthquake void ratios of the hydraulic fill in the upstream shell using the slope of the critical strength line determined from reconstituted specimens. This is shown in Fig. 3 where the after-consolidation void ratios of samples R̄7 and R̄17 [from Castro et al. (1989)] are corrected to a pre-earthquake void ratio of 0.717 and 0.688, respectively. The resulting undrained critical strengths for samples R̄7 and R̄17 are 45 and 40 kPa (940 and 835 psf), respectively. The range of undrained critical strength in the upstream shell prior to the 1971 earthquake for all undisturbed samples is 7–96 kPa (145–2,000 psf). The 33rd percentile value of 20–30 kPa (415–625 psf) was then selected to represent the undrained critical strength of the weakest layers, which are believed to have dominated the liquefaction of the upstream shell during the 1971 earthquake (Marcuson et al. 1990).

The after-consolidation void ratio of the undisturbed test specimens was adjusted to account for void-ratio changes due to excavation of the exploration shaft, sampling, specimen preparation, in situ densification between 1971 and 1985 as well as during the 1971 earthquake shaking, and the difference between the void ratios of the upstream and downstream hydraulic fill. It is quite obvious that the success of this laboratory testing approach depends on the uncertain accuracy with which the in situ void ratio is determined and the uniqueness of the undrained critical-strength line. A sufficient number of specimens must be tested to define the position of the critical strength line of undisturbed specimens for the range of gradation and fines content encountered in the deposit.

Critical Strength from Case Histories and Standard Penetration Resistance

Seed (1987) has presented an alternative approach for estimating the undrained critical strength of liquefied soils based on field case histories. This approach is based on the results of back-analysis of liquefaction case histories where values of the undrained critical strength were calculated for soil zones in which standard penetration test (SPT) results were available. It should be noted that the values of s_u(critical) were back-calculated using limit equilibrium analyses, the final geometry of the slide mass, and different failure surfaces to determine a lower-bound critical strength. Seed and Harder (1990) used these data to develop the relationship between the undrained critical strength mobilized during postliquefaction flow, s_u(critical, mob), and equivalent clean sand blow count, $(N_1)_{60\text{-}cs}$, shown in Fig. 4.

The equivalent clean sand blow count is a "standard" SPT blow count based on standardized equipment and procedures as described by Seed et al. (1985). The standardized equipment results in a transfer of approximately 60% of the theoretical free-fall hammer energy to the drill stem. This results in a field blow count termed N_{60}. The value of $(N_1)_{60}$ corresponds to the equivalent penetration resistance at an effective overburden stress of 100 kPa (1 ton/sq ft). The field blow count is corrected to 100 kPa (1 tons/sq ft) using the following expression:

$$(N_1)_{60} = C_N \times N_{60} \quad \text{(1)}$$

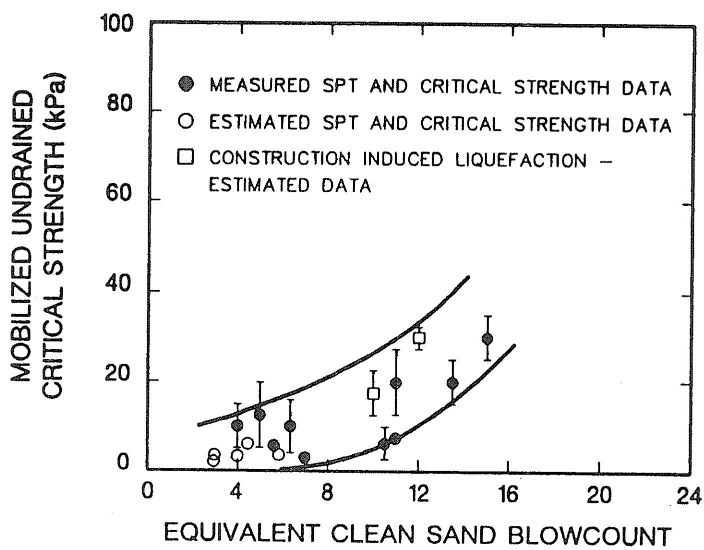

FIG. 4. Relationship between Undrained Critical Strength from Case Histories and Blow Count [from Seed and Harder (1990)]

where C_N = the overburden correction factor. Seed et al. (1985) recommended two relationships between C_N and the initial effective vertical stress, σ'_{vo}, based on data from the Waterways Experiment Station (Marcuson and Bieganousky 1977). One relationship corresponds to a relative density of 40–60%, and the other corresponds to a relative density of 60–80%. Liao and Whitman (1985) have proposed the following relationship:

$$C_N = \frac{1}{(\sigma'_{vo})^{1/2}} \qquad (2)$$

where σ'_{vo} is expressed in tons per square foot (kilogram per square centimeter). Eq. (2) is in good agreement with the relationships presented by Seed et al. (1985), and it eliminates the need to estimate the relative density. The value of $(N_1)_{60}$ is corrected for fines content to generate an equivalent clean sand blow count as follows:

$$(N_1)_{60\text{-}cs} = (N_1)_{60} + \Delta(N_1)_{60} \qquad (3)$$

where $\Delta(N_1)_{60}$ = a function of the percent fines, i.e., the percent passing the No. 200 sieve, as shown in Table 1. Table 1 shows that the critical-strength fines-content correction proposed by Seed (1987) is smaller than that for the yield, or triggering liquefaction, strength correction proposed by Seed et al. (1985).

Undrained Critical Strength Expressed as Strength Ratio

Fig. 5 shows a relationship between the undrained critical-strength ratio mobilized during postliquefaction flow, s_u(critical, mob)/σ'_{vo}, and $(N_1)_{60\text{-}cs}$. This relationship is similar to that shown in Fig. 4 except s_u(critical, mob) is presented in a dimensionless form and is based on an increased number of case histories. Normalizing s_u(critical, mob) with σ'_{vo} will aid stability analyses of the upstream and downstream slopes of existing dams. A similar approach of s_u(critical, mob)/σ'_{vo} against $(N_1)_{60\text{-}cs}$ has been reported by Jefferies et al. (1990). The numbers adjacent to the data points in Fig. 5 correspond to the case history numbers shown in Table 2. Table 3 presents references for the case histories in Table 2.

For comparison purposes, the s_u(critical, mob)/σ'_{vo} versus $(N_1)_{60\text{-}cs}$ data were recalculated using the yield strength fines-content correction instead of the critical-strength fines-content correction. Table 2 shows that the yield-strength fines-content correction increased the value of $(N_1)_{60\text{-}cs}$ for 11 of

TABLE 1. Values of $\Delta(N_1)_{60}$ from Seed et al. (1985) and Seed (1987)

Fines content (%) (1)	Yield strength, $\Delta(N_1)_{60}$ (2)	Critical strength, $\Delta(N_1)_{60}$ (3)
10	2.5	1
15	4	—
20	5	—
25	6	2
30	6.5	—
35	7	—
50	7	4
75	7	5

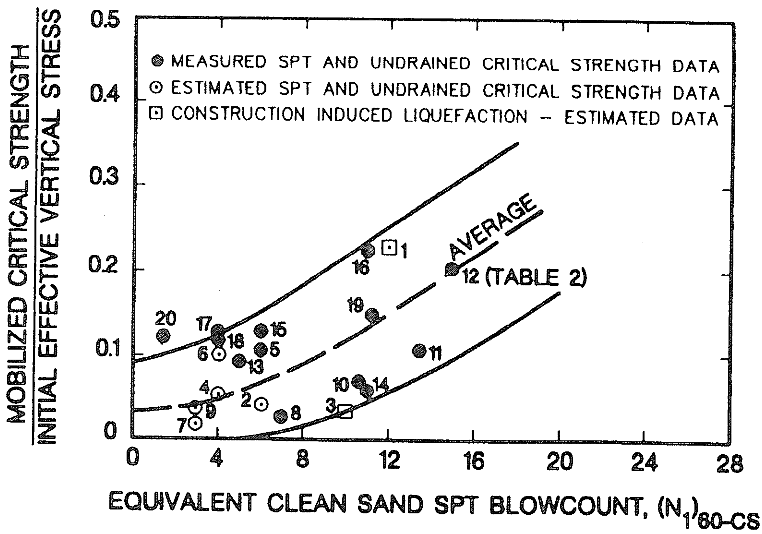

FIG. 5. Relationship between Undrained Critical Strength Ratio and Equivalent Clean Sand Blow Count Based on Critical Strength Fines-Content Correction

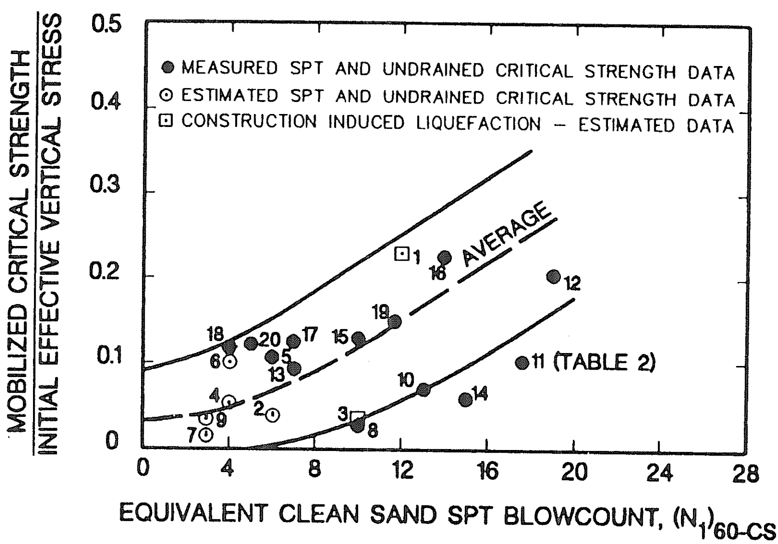

FIG. 6. Relationship between Undrained Critical Strength Ratio and Equivalent Clean Sand Blow Count Based on Yield Strength Fines-Content Correction

the 20 case histories. Fig. 6 shows that the revised values of s_u(critical, mob)/σ'_{vo} against $(N_1)_{60\text{-}cs}$ do not differ significantly from the boundary lines developed in Fig. 5 using the critical strength fines-content correction. As a result, the proposed procedure for estimating s_u(critical)/σ'_{vo} will use the yield-strength fines-content correction.

The undrained critical-strength ratio was calculated using the initial ef-

TABLE 2. Case Histories Used to Develop Relationship between Mobilized Undrained Critical Strength Ratio and Corrected Penetration Resistance

Case history (1)	Structure (2)	Apparent cause of sliding (3)	Average measured $(N_1)_{60}$ (blows/ft) (4)	Average fines content (%) (5)	$(N_1)_{60\text{-}cs}$ using critical fines correction (blows/ft) (6)	$(N_1)_{60\text{-}cs}$ using yield fines correction (blows/ft) (7)	Average undrained critical shear strength (psf) (8)	Effective overburden stress at middle of liquefied layer (psf) (9)	Average critical strength ratio (10)
1	Calaveras Dam	1918 Construction	—	—	12[a]	12[a]	650 ± 50	2,855	0.228
2	Sheffield Dam	1925 Santa Barbara earthquake (M = 6.3)	—	—	6[a]	6[a]	75 ± 25	1,975	0.038
3	Fort Peck Dam	1938 Construction	—	—	10[a]	10[a]	350 ± 100	10,815	0.032
4	Solfatara Canal Dike	1940 El Centro earthquake (M = 7.2)	—	—	4[a]	4[a]	50 ± 25	955	0.052
5	Lake Merced Bank	1957 San Francisco earthquake (M = 5.7)	6	3	6	6	100	950	0.105
6	Kwagishi-Cho Building	1964 Niigata earthquake (M = 7.5)	—	—	4[a]	4[a]	120	1,225	0.098
7	Uetsu Railway Embankment	1964 Niigata earthquake (M = 7.5)	—	—	3[a]	3[a]	40	2,690	0.015
8	Snow River Bridge Fill	1964 Alaskan earthquake (M = 8.5)	5	10–30	7	10	50	2,100	0.024
9	Koda Numa Highway Embankment	1968 Tokachi-Oki earthquake (M = 7.9)	—	—	3[a]	3[a]	50	1,550	0.032
10	San Fernando Juvenile Hall	1971 San Fernando earthquake (M = 6.6)	6	65	10.5	13	130 ± 70	1,940	0.067
11	Lower San Fernando Dam	1971 San Fernando earthquake (M = 6.6)	11.5	25–30	13.5	17.5	400 ± 100	3,930	0.102
12	Upper San Fernando Dam	1971 San Fernando earthquake (M = 6.6)	13	25	15	19	600 ± 100	2,975	0.202

13	Mochi-koshi Tailings Dams	1978 Izu-Oshima earthquake (M = 7.0)	0	80	5	7	250 ± 150	2,715	0.092
14	Whiskey Springs Fan	1983 Borah Peak earthquake (M = 7.3)	8[b]	40[b]	11	15	150 ± 10	2,630	0.057
15	La Marquesa Dam—upstream slope	1985 Chilean earthquake (M = 7.8)	4	30	6	10	200 ± 120	1,600	0.125
16	La Marquesa Dam—downstream slope	1985 Chilean earthquake (M = 7.8)	9	20	11	14	400 ± 150	1,790	0.224
17	La Palma Dam	1985 Chilean earthquake (M = 7.8)	3	15	4	7	200 ± 100	1,670	0.120
18	Lake Ackerman	From seismic reflection survey	3	0–5	4	4	215 ± 45	1,845	0.117
19	Nerlerk Embankment	1990 construction	10–11	0–10	11–11.5	10–12.5	NA	NA	0.148
20	Heber Road	1979 Imperial Valley earthquake	1	15	1.5	5	100	800	0.125

[a]SPT blow count estimated from appraisal of relative density.
[b]Equivalent SPT blow count determined from Becker penetration test performed in silty gravel; fine-material content computed for −10-mm sizes.
Note: 1 psf = 0.04788 kPa.

TABLE 3. Case Histories Used to Develop Relationship between Mobilized Undrained Critical Strength Ratio and Corrected Penetration Resistance

Case history (1)	Structure (2)	Reference (3)
1	Calaveras Dam	Hazen (1918)
2	Sheffield Dam	Seed et al. (1969)
3	Fort Peck Dam	Casagrande (1965); Middlebrooks (1942)
4	Solfatara Canal Dike	Ross (1968); Seed (1987)
5	Lake Merced Bank	Ross (1968); Seed (1987)
6	Kwagishi-Cho Building	Seed (1987); Yamada (1966)
7	Uetsu Railway Embankment	Seed (1987); Yamada (1966)
8	Snow River Bridge Fill	Ross et al. (1969)
9	Koda Numa Highway Embank.	Mushima and Kimura (1970)
10	San Fernando Juvenile Hall	Bennett (1989)
11	Lower San Fernando Dam	Seed et al. (1975), 1989
12	Upper San Fernando Dam	Seed et al. (1975)
13	Mochi-Koshi Tailings Dams	Marcuson et al. (1979)
14	Whiskey Springs Fan	Harder (1988)
15	La Marquesa Dam—U/S slope	De Alba et al. (1987)
16	La Marquesa Dam—D/S slope	De Alba et al. (1987)
17	La Palma Dam	De Alba et al. (1987)
18	Lake Ackerman	Hryciw et al. (1990)
19	Nerlerk Embankment	Jefferies et al. (1990); Rogers et al. (1990)
20	Heber Road	Davis et al. (1988); Reyna and Chameau (1991)

fective vertical stress at the middepth of the layer that was reported as having liquefied. It is important to note that the pre-earthquake geometry was used to estimate σ'_{vo}, while the final geometry of the slide mass was used to estimate s_u(critical, mob). The calculation of σ'_{vo} is illustrated using La Marquesa Dam in Chile (De Alba et al. 1987). La Marquesa Dam had a pre-earthquake maximum height of 10 m (30 ft), a crest length of 220 m (660 ft), and a storage capacity of 204,000 m^3 (227,000 cu ft). During the March 3, 1985, earthquake, the dam experienced major slides in the upstream and downstream slopes. Horizontal displacements in the zone of greatest damage reached approximately 11 m (33 ft) at the toe of the upstream slope and 6.5 m (20 ft) at the toe of the downstream slope.

Fig. 7 shows a cross section through the failed portion of La Marquesa Dam. It can be seen that the $(N_1)_{60}$ values of the silty sand layer on which the dam was constructed are low. De Alba et al. (1987) concluded that this silty sand layer liquefied under the upstream and downstream slopes causing the observed movements. The average effective vertical stress in the silty sand beneath the upstream slope was calculated to be 77 kPa (1,600 psf), and the average effective vertical stress in the silty sand beneath the downstream slope was estimated to be 86 kPa (1,790 psf). The values of s_u(critical, mob)/σ'_{vo} were then calculated for the upstream and downstream slopes using the critical strengths back-calculated by Seed and Harder (1990).

Comparison of Mobilized Yield and Critical-Strength Ratios

Fig. 8 shows the relationship between seismic shear stress ratio and $(N_1)_{60\text{-}cs}$ for earthquakes of magnitude of 7.5 (Seed et al. 1985). The

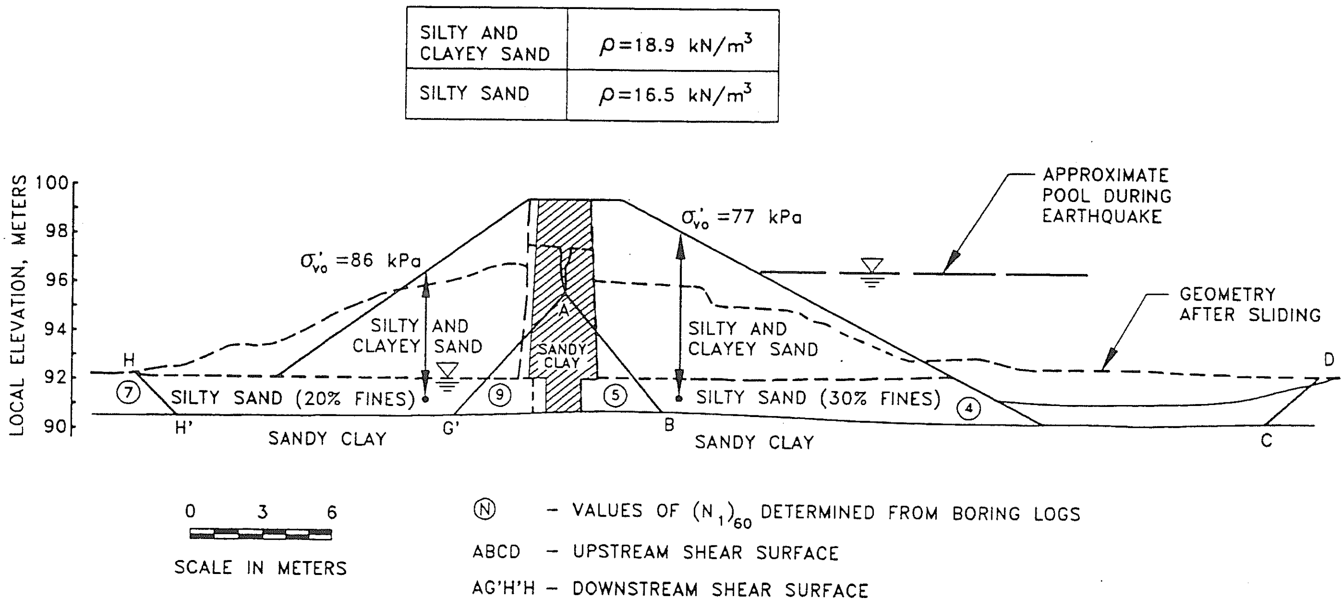

FIG. 7. Reconstructed Cross Section through Failed Portion of La Marquesa Embankment [from De Alba et al. (1987)]

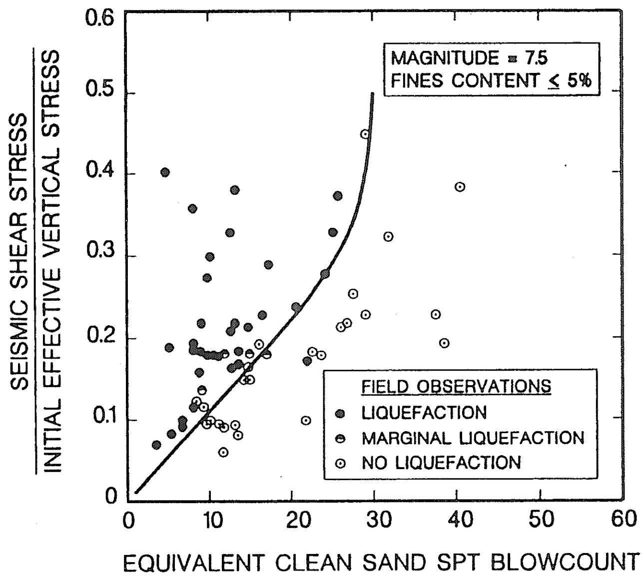

FIG. 8. Relationship between Seismic Shear Stress Ratio Triggering Liquefaction and Equivalent Clean Sand Blow Count for M = 7.5 Earthquakes [from Seed et al. (1985)]

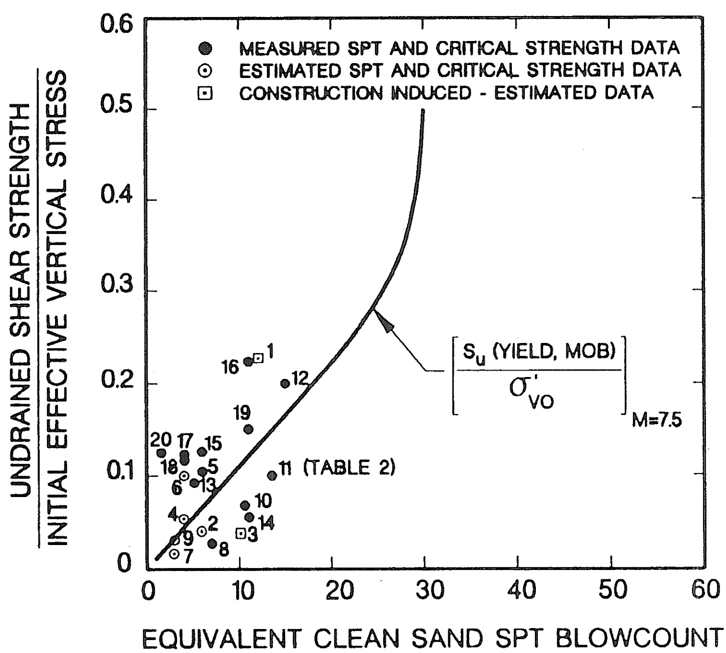

FIG. 9. Comparison of Undrained Critical and Yield Strength Ratios Back-Calculated from Field Case Histories

line in Fig. 8 separates field conditions causing liquefaction from conditions not causing liquefaction in clean sands. Since the yield strength controls the triggering of liquefaction, the seismic shear stress ratios corresponding to the boundary line in Fig. 8 are the undrained yield-strength ratios mobilized in the field, $s_u(\text{yield, mob})/\sigma'_{vo}$, for a given value of $(N_1)_{60\text{-}cs}$. A relationship between $s_u(\text{yield, mob})/\sigma'_{vo}$ and $(N_1)_{60\text{-}cs}$, for $(N_1)_{60\text{-}cs} \leq 20$, can be defined by the line that separates liquefiable and nonliquefiable clean sands for an earthquake magnitude of 7.5 as follows:

$$\frac{s_u(\text{yield, mob})}{\sigma'_{vo}} = 0.011 \times (N_1)_{60\text{-}cs} \quad \text{(4)}$$

The undrained critical-strength ratio data in Fig. 5 are compared with $s_u(\text{yield, mob})/\sigma'_{vo}$ for a magnitude of 7.5 in Fig. 9. A large number of $s_u(\text{critical, mob})/\sigma'_{vo}$ data points plot above the $s_u(\text{yield, mob})/\sigma'_{vo}$ against $(N_1)_{60\text{-}cs}$ relationship. This suggests that in a large number of cases, significant drainage occurred during postliquefaction flow, and by the time the liquefied mass came to rest, $s_u(\text{critical, mob})$ was actually equal to or greater than $s_u(\text{yield, mob})$. In other words, a steady state of deformation at constant volume, constant effective normal stress, constant shear stress, and constant velocity may not exist during flow of liquefied sand in the field. Table 2 shows that the critical-strength ratios lying significantly below the $s_u(\text{yield, mob})/\sigma'_{vo}$ curve correspond to soils with fines-content contents greater than 30%–40%. Therefore, material that has a fine content greater than 30–40% will undergo little or no drainage during flow of the liquefied mass. It should be noted that loose sands exhibit some strength gain, i.e., dilation, at large strains (see Fig. 1). This dilation may also have contributed to the observed strength gain during post-liquefaction flow. However, the primary factor appears to be drainage of the liquefied mass.

New Approach for Estimating Undrained Critical Strength

For seismic stability analyses of an existing slope, drainage of the slide mass during post-liquefaction flow cannot be assumed. Therefore, a value of $s_u(\text{critical})$ corresponding to constant volume or an undrained condition and the original slope geometry must be used in stability analyses. In other words, the stability of the original slope configuration at the instant of liquefaction is determined by the constant volume $s_u(\text{critical})$, rather than the back-calculated partially drained $s_u(\text{critical, mob})$. Therefore, a technique for estimating constant volume $s_u(\text{critical})$ using $(N_1)_{60\text{-}cs}$ was sought from undrained laboratory test results.

The main difficulty in developing a relationship between $s_u(\text{critical})/\sigma'_{vo}$ and $(N_1)_{60\text{-}cs}$ was estimating the value of $(N_1)_{60\text{-}cs}$ corresponding to the laboratory values of $s_u(\text{yield})$ and $s_u(\text{critical})$. It was decided to use the correlation between $s_u(\text{yield, mob})/\sigma'_{vo}$ and $(N_1)_{60\text{-}cs}$ in Fig. 8 or (4) to estimate the value of $(N_1)_{60\text{-}cs}$ corresponding to $s_u(\text{yield})$ at 15 equivalent cycles in a cyclic simple shear test. An equivalent number of uniform stress cycles equal to 15 in a cyclic simple shear test was assumed to simulate the field stress conditions of a magnitude 7.5 earthquake as proposed by Seed (1979). If $s_u(\text{critical})$ and $s_u(\text{yield})$ are measured in a cyclic simple shear test at the same relative density and test conditions, the value of $(N_1)_{60\text{-}cs}$ corresponding to $s_u(\text{yield})$ should also correspond to $s_u(\text{critical})$. Therefore, a relationship between $s_u(\text{critical})/\sigma'_{vo}$ and $(N_1)_{60\text{-}cs}$ could be obtained for use in stability analyses.

To verify this approach, it was necessary to compare laboratory measurements of s_u(yield) and the corresponding measurements of $(N_1)_{60\text{-}cs}$ to the field performance data for an earthquake magnitude of 7.5 in Fig. 8. Such a comparison has been made by Tokimatsu (1988) using undrained cyclic triaxial test data at 15 equivalent cycles on high-quality specimens of clean sands. The high-quality undisturbed specimens were obtained by in situ freezing and coring method. The specimens were thawed and consolidated under an equal all-around pressure equal to the in situ σ'_{vo} before they were subjected to a sinusoidal axial load of constant amplitude at a frequency of 0.1 Hz. These results, together with additional cyclic triaxial test data from Ishihara and Koga (1981), are shown in Fig. 10. The cyclic triaxial test results were corrected to simple shear mode using the correction factor C_r, developed by De Alba et al. (1975) as described subsequently. The laboratory yield strength data from high-quality undisturbed specimens subjected to in situ σ'_{vo} before shear are consistent with the s_u(yield, mob)/σ'_{vo} against $(N_1)_{60\text{-}cs}$ relationship developed by Seed et al. (1985) based on field case histories of liquefaction during earthquakes. Therefore, estimating the values of $(N_1)_{60\text{-}cs}$ corresponding to the laboratory value of s_u(yield)/σ'_{vo} measured at 15 equivalent cycles and applying it to s_u(critical)/σ'_{vo} appears acceptable.

Values of s_u(yield) and s_u(critical) from laboratory cyclic triaxial tests, s_u(yield, T), cyclic simple shear tests, s_u(yield, CSS), and torsional shear tests, s_u(yield, TS), were used to establish a relationship between constant volume s_u(critical)/σ'_{vo} and $(N_1)_{60\text{-}cs}$. Fig. 11 shows that only five references were located in the literature in which s_u(yield) and s_u(critical) were mea-

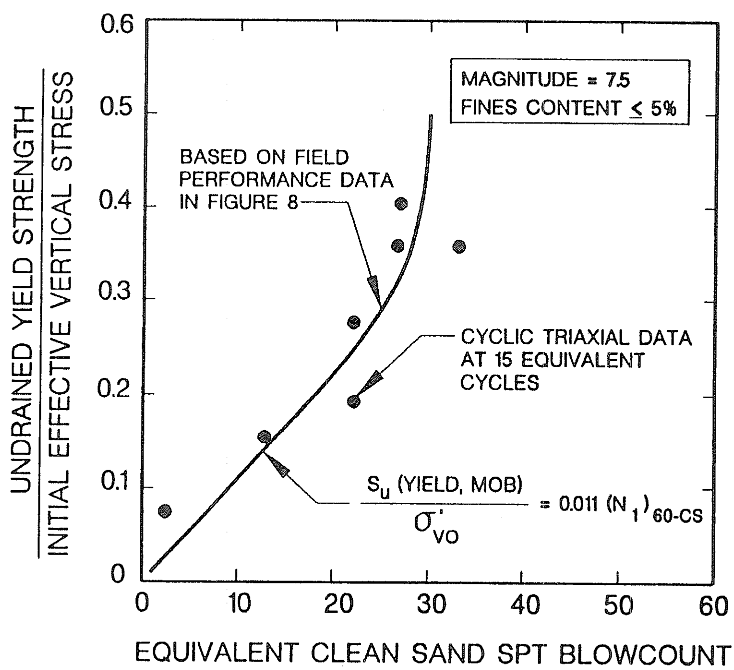

FIG. 10. Comparison of Field and Laboratory Yield Strength Ratios [data from Tokimatsu (1988) and Ishihara and Koga (1981)]

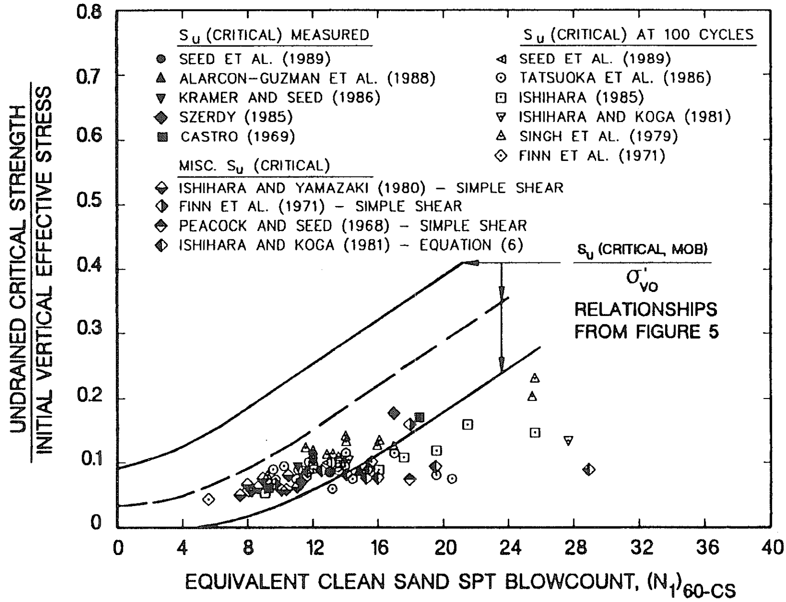

FIG. 11. Comparison of Undrained Critical Strength Ratios from Field Performance and Laboratory Shear Tests

sured directly (solid data symbols). These data were obtained from cyclic triaxial compression tests, except for the data presented by Alarcon-Guzman et al. (1988), which was obtained using torsional shear tests. For reference, the upper, lower, and average relationships of s_u(critical, mob)/σ'_{vo} from Fig. 5 are included in Fig. 11. As expected, the constant volume values of s_u(critical) obtained from laboratory tests plot near or below the lower bound of the s_u(critical, mob)/σ'_{vo} data.

The cyclic triaxial test results were corrected to simple shear mode using the correction factor C_r developed by De Alba et al. (1975). The value of C_r near 15 equivalent cycles, i.e., an earthquake magnitude of 7.5, is 0.64 and decreases to approximately 0.57 for 100 or more cycles. The cyclic triaxial yield strength ratios, s_u(yield, T)/σ'_{1c}, were corrected to the cyclic simple shear yield strength ratio, s_u(yield, CSS)/σ'_{vc}, using the following expression:

$$\frac{s_u(\text{yield, CSS})}{\sigma'_{vc}} = C_r \times \frac{s_u(\text{yield, T})}{\sigma'_{1c}} \quad \text{(5)}$$

where σ'_{1c} = the consolidation pressure in the triaxial test; and σ'_{vc} = the vertical consolidation pressure in the simple shear test. The torsional shear test results were not corrected using C_r.

Since the data base of test results in which both the yield and critical strengths were measured is limited, the yield strength after 100 or more stress cycles was assumed to be equal to the critical strength. After 100 or more cycles, the cyclic stress ratio usually levels off, as shown by typical data in Fig. 12 from cyclic triaxial tests on undisturbed hydraulic fill from the Lower San Fernando Dam. Seed et al. (1989) measured the critical-

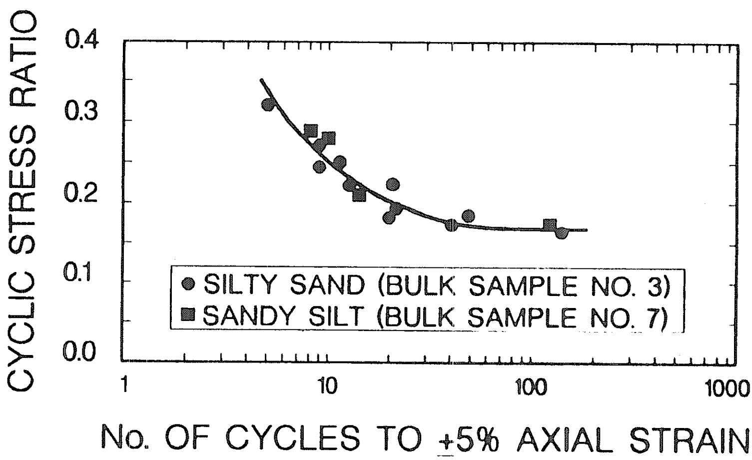

FIG. 12. Results of Cyclic Triaxial Tests on Undisturbed Hydraulic Fill from Lower San Fernando Dam [from Seed et al. (1989)]

strength ratio of the sandy silt, i.e., bulk sample 7, using monotonically loaded, consolidated-undrained triaxial compression tests. The measured critical strength ratios for voids ratios similar to the undisturbed specimens shown in Fig. 12, i.e., 0.624–0.689, ranged from 0.19 to 0.27. Thus, the yield strength ratio at 100 or more cycles may be a reasonable estimate of the critical strength ratio.

From Fig. 12, values of s_u(yield, T) at 15 cycles and s_u(critical, T) at 100 cycles are equal to 0.227 and 0.174, respectively, for the sandy silt. These values were corrected to 0.145 and 0.099 using values of C_r equal to 0.64 and 0.57, respectively. A value of $(N_1)_{60\text{-}cs}$ equal to 13 was obtained from Fig. 8 using the yield-strength ratio of 0.145. The critical-strength ratio is plotted using $(N_1)_{60\text{-}cs} = 13$ in Fig. 11, as well as other data obtained using the same technique. These values of critical-strength ratio are in good agreement with the measured critical strength ratios (solid data symbols).

The values of s_u(yield, CSS) at 15 equivalent cycles and s_u(critical, CSS) at 100 or more equivalent cycles from cyclic simple shear tests (Finn et al. 1971; Ishihara and Yamazaki 1980; Peacock and Seed 1968) are also shown in Fig. 11. The values of s_u(critical)/σ'_{vo} for the cyclic triaxial, torsional shear, and cyclic simple shear tests are in good agreement. To further verify the data in Fig. 11, values of $(N_1)_{60}$ were estimated for after-consolidation relative densities in cyclic triaxial tests using the following relationship presented by Tokimatsu and Seed (1987):

$$(N_1)_{60} = 44 \times D_r^2 \qquad (6)$$

Eq. (6) was developed using field density measurements, in situ freezing of natural deposits for undisturbed sampling to estimate relative density, and Meyerhof's (1957) proposed relationship between relative density, effective overburden pressure, and blow count. This relationship is in agreement with the data presented by Skempton (1986) for freshly deposited sands and reconstituted laboratory specimens of sand. Values of $(N_1)_{60}$ corresponding to after-consolidation relative densities were then corrected for fines content to obtain $(N_1)_{60\text{-}cs}$. This procedure was applied to Ishihara and Koga's (1981) cyclic triaxial data. The results are in good agreement with the previous data shown in Fig. 11.

Fig. 13 shows the data from Fig. 11 (open data symbols) and the recommended relationship to estimate the constant volume value of s_u(critical)/σ'_{vo}. For comparison purposes, the values of s_u(critical, mob)/σ'_{vo} from Fig. 6 (solid data symbols) are also shown in Fig. 13. The straight line through the constant volume s_u(critical)/σ'_{vo} data can be expressed as

$$\frac{s_u(\text{critical})}{\sigma'_{vo}} = 0.0055 \times (N_1)_{60\text{-}cs} \quad (7)$$

Therefore, the undrained critical strength ratio is approximately one-half the yield strength ratio, i.e., (4), for an earthquake magnitude of 7.5.

Eq. (7) forecasts postyield liquefaction-related instability for all cases in Fig. 6 except 3, 8, 10, and 14. The values of $(N_1)_{60\text{-}cs}$ corresponding to the s_u(critical)/σ'_{vo} and s_u(critical, mob)/σ'_{vo} data in Fig. 13 were obtained using the yield strength fines-content correction in Table 1. The yield-strength fines-content correction was used so that the value of $(N_1)_{60\text{-}cs}$ corresponding to s_u(critical) and s_u(yield) was the same. This appears acceptable since only four case histories plotted below (7) in Fig. 13, and Figs. 5 and 6 showed no significant difference between the results of the two fines-content corrections. Therefore, it is proposed that the $(N_1)_{60}$ values used in (4) and (7) to estimate s_u(yield) and s_u(critical) be corrected using the yield-strength fines-content correction.

For the Lower San Fernando Dam, the hydraulic fill that liquefied had an average value of $(N_1)_{60}$ equal to 11.5 (Table 2), and thus $(N_1)_{60\text{-}cs}$ = 17.5 using the yield-strength fines-content correction. Using (7) and σ'_{vo} = 190 kPa (3,930 psf), a value of s_u(critical) is estimated equal to 18 kPa (350 psf). As expected, this value is slightly lower than the average value of 19 kPa (400 psf) back-calculated by Seed and Harder (1990). Since the fines content of the hydraulic fill is 25% (Seed and Harder 1990), some drainage probably occurred during postliquefaction flow of the hydraulic fill, resulting in the slightly higher back-calculated critical strength.

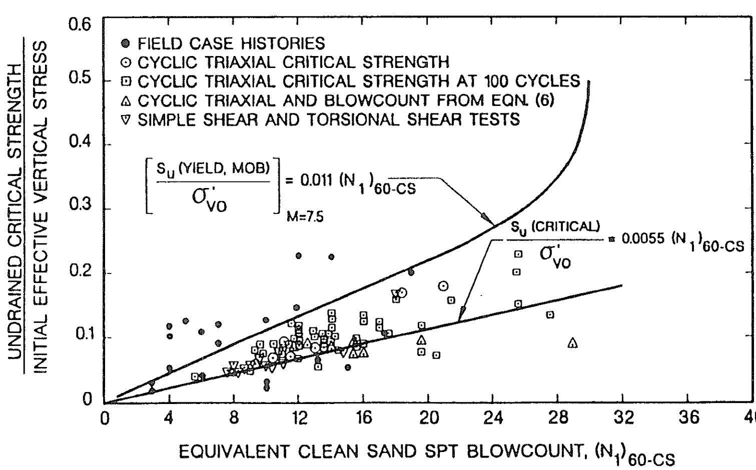

FIG. 13. Relationship between Undrained Critical Strength Ratio and Equivalent Clean Sand Blow Count

Conclusions

The following conclusions are based on the analysis, data, and interpretation presented in this paper:

1. Shear strengths of liquefied soil back-calculated from case histories of liquefaction failure are normalized with respect to preliquefaction effective overburden pressure to determine critical strength ratios.
2. A comparison of these critical strength ratios with back-calculated yield, or triggering liquefaction, strength ratios suggests that in a majority of the case histories, significant drainage may have taken place during post-yield flow of the liquefied soil. Postliquefaction stability analyses cannot assume drainage and must be based on a constant volume critical strength.
3. A constant-volume critical-strength ratio is estimated using an equivalent clean sand SPT blow count and (7). The yield-strength fines-content correction (Table 1) is used to correct the silty sand blow count when estimating both the yield and critical strength ratios. The constant volume critical strength is then calculated for values of effective vertical stress in the zone of liquefaction to evaluate stability of the original slope configuration.
4. Alternatively, a sampling and laboratory testing program can be carried out. Values of yield strength ratio at 15 equivalent cycles, i.e., an earthquake magnitude of 7.5, and critical strength ratio are measured using cyclic triaxial, cyclic simple shear, and/or cyclic torsional shear tests. The results of cyclic triaxial tests should be corrected, using $C_r = 0.64$, to the simple shear test condition. Using the yield strength ratios measured at 15 equivalent cycles and (4), a relationship between the undrained critical strength ratio and the equivalent clean sand SPT blow count is established. The constant volume critical strength ratio can then be determined from this relationship using the measured equivalent clean sand SPT blow counts. This approach does not require an accurate knowledge of the in situ void ratio of sand.

Acknowledgments

This study was performed as a part of National Science Foundation grant BCS-9196074. The support of this agency is gratefully acknowledged.

Appendix. References

Alarcon-Guzman, A., Leonards, G. A., and Chameau, J. L. (1988). "Undrained monotonic and cyclic strength of sands." *J. Geotech. Engrg.*, ASCE, 116(6), 1089-1109.

Bennett, M. J. (1989). "Liquefaction analysis of the 1971 ground failure at the San Fernando Valley Juvenile Hall, California." *Bull. Assoc. of Engrg. Geol.*, 26(2), 209–226.

Casagrande, A. (1936). "The shearing characteristics of soils and its relation to the stability of earth dams." *J. Boston Soc. of Civ. Engrs.*, Jan., 257–276.

Casagrande, A. (1965). "The role of the 'calculated risk' in earthwork and foundation engineering." *J. Soil Mech. Found. Engrg. Div.*, ASCE, 91(4) 1–40.

Castro, G. (1969). "Liquefaction of sands." *Harvard Soil Mechanics Series No. 81*, Harvard Univ., Cambridge, Mass.

Castro, G., Keller, T. O., and Boynton, S. S. (1989). "Re-evaluation of the Lower

San Fernando Dam: An investigation of the February 9, 1971 slide." *Contract Report D-89-2, Report 1*, Vols. 1 and 2, U.S. Army Engineer Wtrways. Experiment Station, Vicksburg, Miss.
Davis, A. P., Castro, G., and Poulos, S. J. (1988). "Strengths backfigured from liquefaction case histories." *Proc. 2nd Inst. Conf. on Case Histories in Geotech. Engrg.*, University of Missouri at Rolla, 4, 1693–1701.
De Alba, P., Chan, C. K., and Seed, H. B. (1975). "Determination of soil liquefaction characteristics by large-scale laboratory tests." *Report No. UCB/EERC-75-14*, Earthquake Engrg. Res. Ctr., Univ. of California, Berkeley, Calif.
De Alba, P., Seed, H. B., Retamal, E., and Seed, R. B. (1987). "Residual strength of sand from dam failures in the Chilean earthquake of March 3, 1985." *Report No. UCB/EERC-87-11*, Earthquake Engrg. Res. Ctr., Univ. of California, Berkeley, Calif.
Dennis, N. D. (1988). "Influence of specimen preparation techniques and testing procedure on undrained steady state shear strength." *Proc. Advanced Triaxial Testing of Soils and Rock (ASTM STP 977)*, Am. Soc. for Testing and Mater., Philadelphia, Pa., 642–654.
Finn, W. D. L., Pickering, D. J., and Bransby, P. L. (1971). "Sand liquefaction in triaxial and simple shear tests." *J. Soil Mech. Found. Engrg. Div.*, ASCE, 97(4), 639–659.
Harder, L. F. (1988). "Use of penetration tests to determine the cyclic loading resistance of gravelly soils during earthquake shaking," PhD thesis, University of California, Berkeley, Calif.
Hazen, A. (1918). "A study of the slip in the Calaveras Dam." *Eng. News Rec.*, 81(26), 1158–1164.
Hryciw, R. D., Vitton, S., and Thomann, T. G. (1990). "Liquefaction and flow failure during seismic exploration." *J. Geotech. Engrg.*, ASCE 116(12), 1881–1899.
Ishihara, K. (1985). "Stability of natural deposits during earthquakes." *Proc. 11th Int. Conf. on Soil Mech. and Found. Engrg.*, International Society of Soil Mechanics and Foundation Engineering, 1, 321–376.
Ishihara, K., and Koga, Y. (1981). "Case studies of liquefaction in the 1964 Niigata earthquake." *Soils Found.*, 21(3), 35–52.
Ishihara, K., and Yamazaki, F. (1980). "Cyclic simple shear tests on saturated sand in multi-directional loading." *Soils Found.*, 20(1), 45–59.
Jefferies, M. G., Been, K., and Hachey, J. E. (1990). "Influence of scale on the constitutive behavior of sand." *Proc. Canadian Geotech. Engrg. Conf.*, Laval University, 1, 263–273.
Konrad, J.-M. (1990a). "Minimum undrained strength of two sands." *J. Geotech. Engrg.*, ASCE, 116(6), 932–947.
Konrad, J.-M. (1990b). "Minimum undrained strength versus steady-state strength of sands." *J. Geotech. Engrg.*, ASCE, 116(6), 948–963.
Kramer, S. L., and Seed, H. B. (1988). "Initiation of soil liquefaction under static loading conditions." *J. Geotech. Engrg.* ASCE, 114(4), 412–430.
Liao, S. C., and Whitman, R. V. (1985). "Overburden correction factors for SPT in sand." *J. Geotech. Engrg.*, ASCE, 112(3), 373–377.
Marcuson, W. F., III, Ballard, R. F., Jr., and Ledbetter, R. H. (1979). "Liquefaction failure of tailings dams resulting from the Near Izu Oshima earthquake, 14 and 15 January, 1978." *Proc. 6th Pan-American Conf. on Soil Mech. and Found. Engrgs.*, 2, BiTech Publishing, Lima, Peru, 69–80.
Marcuson, W. F., III, and Biganousky, W. A. (1977). "Laboratory standard penetration tests on fine sands." *J. Geotech. Engrg. Div.*, ASCE, 103(6), 565–588.
Marcuson, W. M., Hynes, M. E., and Franklin, A. G. (1990). "Evaluation of use of residual strength in the seismic stability of embankments." *Earthquake Spectra*, 6(3), 529–572.
Meyerhof, G. G. (1957). Discussion of "Research on determining the density of sands by spoon penetration testing," by H. J. Gibbs and W. G. Holtz. *Proc. 4th Int. Conf. on Soil Mech. and Found. Engrg.*, International Society of Soil Mechanics and Foundation Engineering, 3, 110.

Middlebrooks, T. A. (1942). "Fort Peck slide." *Trans.*, 107, 723–764.
Mushima, S., and Kimura, H. (1970). "Characteristics of landslides and embankment failures during the Tokachi-Oki earthquake." *Soils Found.*, 10(2), 39–51.
Peacock, W. H., and Seed, H. B. (1968). "Sand liquefaction under cyclic loading simple shear conditions." *J. Soil Mech. Found. Engrg. Div.*, ASCE, 94(3), 689–708.
Poulos, S. J., Castro, G., and France, W. (1985). "Liquefaction evaluation procedure." *J. Geotech. Engrg.*, ASCE, 111(6), 772–792.
Reyna, F., and Chameau, J. L. (1991). "Statistical evaluation of CPT and DMT measurements at the Heber Road site." *Proc. ASCE Foundation Congress*, ASCE, 1, 14–25.
Rogers, B. T., Been, K., Hardy, M., Johnson, G., and Hachey, J. (1990). "Re-analysis of Nerlerk B-67 berm failures." *Proc. Canadian Geotech. Engrg. Conf.*, Laval University, 1, 227–237.
Ross, G. A. (1968). "Case studies of soil stability problems resulting from earthquakes," PhD thesis University of California, Berkeley, Calif.
Ross, G. A., Seed, H. B., and Migliaccio, R. R. (1969). "Bridge foundations in Alaska foundation." *J. Soil Mech. Found. Engrg. Div.*, ASCE, 95(4), 1007–1036.
Seed, H. B. (1979). "Soil liquefaction and cyclic mobility evaluation for level ground during earthquakes." *J. Geotech. Engrg. Div.*, ASCE, 105(2), 201–255.
Seed, H. B. (1987). "Design problems in soil liquefaction." *J. Geotech. Engrg.*, ASCE, 113(8), 827–845.
Seed, H. B., Lee, K. L., and Idriss, I. M. (1969). "Analysis of Sheffield Dam failure." *J. Soil Mech. Found. Engrg. Div.*, ASCE, 95(6), 1453–1490.
Seed, H. B., Lee, K. L., Idriss, I. M., and Makdisi, F. (1975). "Dynamic analysis of the slide in the Lower San Fernando Dam during the earthquake of February 9, 1971." *J. Soil Mech. Found. Engrg. Div.*, ASCE, 101(9), 889–912.
Seed, H. B., Seed, R. B., Harder, L. F., and Jong, H. L. (1989). "Re-evaluation of the Lower San Fernando Dam: Examination of the post-earthquake slide of February 9, 1971." *Contract Report GL-89-2, Report 2*, U.S. Army Corps of Engrs. Wtrways. Experiment Station, Vicksburg, Miss.
Seed, H. B., Tokimatsu, K., Harder, L. F., and Chung, R. (1985). "Influence of SPT procedures in soil liquefaction resistance evaluations." *J. Geotech. Engrg.*, ASCE, 111(12), 861–878.
Seed, R. B., and Harder, L. F. (1990). "SPT-based analysis of cyclic pore pressure generation and undrained residual strength." *Proc. H. B. Seed Memorial Symp.*, BiTech Publishing, Vancouver, British Columbia, Canada, 2, 351–376.
Singh, S., Seed, H. B., and Chan, C. K. (1979). "Undisturbed sampling and cyclic load testing of sands." *Report No. UCB/EERC-79-33*, Earthquake Engrg. Res. Ctr., Univ. of California, Berkeley, Calif.
Skempton, A. W. (1986). "Standard penetration test procedures and the effects in sands of overburden pressure, relative density, particle size, ageing, and overconsolidation." *Geotechnique*, London, England, 36(3), 425–447.
Szerdy, F. S. (1985). "Flow slide failures associated with low level vibrations," PhD thesis, the University of California, Berkeley, Calif.
Tatsuoka, F., Toki, S., Miura, S., Kato, H., Okamota, M., Yamada, S.-I., Yasuda, S., and Tanizawa, F. (1986). "Some factors affecting cyclic undrained triaxial strength of sands." *Soils Found.*, 26(3), 99–116.
Tokimatsu, K. (1988). "Penetration tests for dynamic problems." *Proc. Int. Symp. on Penetration Testing*, International Society of Soil Mechanics and Foundation Engineering, 1, 117–136.
Tokimatsu, K., and Seed, H. B. (1987). "Evaluation of settlements in sands due to earthquake shaking." *J. Geotech. Engrg.*, ASCE, 113(8), 861–878.
Vaid, Y. P., and Chern, J. C. (1985). "Cyclic and monotonic undrained response of saturated sands." *Advances in the art of testing soils under cyclic conditions (ASCE Annual Convention)*, ASCE, 120–147.
Vaid, Y. P., Chung, E. K. F., and Kuerbis, R. H. (1990). "Stress path and steady state." *Can. Geotech. J.*, 27(1), 1–7.
Vasquez-Herrera, A., and Dobry, R. (1989). "Re-evaluation of the Lower San

Fernando Dam: The behavior of undrained contractive sand and its effect on seismic liquefaction flow failures of earth structures." *Contract Report D-89-2, Report 3*, U.S. Army Engr. Wtrways. Experiment Station, Vicksburg, Miss.

Yamada, G. (1966). "Damage to earth structures and foundation by the Niigata earthquake, June 16, 1964." *Soils Found.*, 6(1), 1–13.